A gonadotropin-releasing hormone type neuropeptide with a high affinity binding site for copper(II) and nickel(II).

Kevin K. Tran[1], Bhawantha M. Jayawardena[1], Maurice R. Elphick[2*] and Christopher E. Jones[1*].

1. The School of Science and Health, Western Sydney University, Locked bag 1797, Penrith, 2759, NSW, Australia. 2. School of Biological & Chemical Sciences, Queen Mary University of London, Mile End Road, London, E1 4NS, United Kingdom.

* Corresponding authors
Christopher E. Jones
The School of Science and Health
Western Sydney University
Locked bag 1797
Penrith, 2759, NSW
Australia.
c.jones@westernsydney.edu.au

Maurice R. Elphick
Queen Mary University of London
Mile End Road
London, E1 4NS
United Kingdom
m.r.elphick@qmul.ac.uk

Table of Contents Entry

Gonadotropin releasing hormone from *Asterias rubens* binds Cu(II) in a nitrogen-rich, high-affinity site. Cu(II)-binding is an evolutionarily conserved feature of GnRH-type neuropeptides.

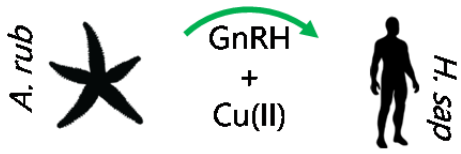

Abstract

In vertebrates gonadotropin-releasing hormone I (GnRH-I) is a key regulator of reproductive development and function. The receptor-binding activity of human GnRH-I can be modified by the presence of divalent copper. Thus, copper binding to N-terminal amino acids in GnRH-I induces structural changes that influence receptor interactions and downstream intracellular signalling cascades. It is not known if copper-binding is restricted to human GnRH-I or if it is also a feature of GnRH-type peptides that have been identified in other taxa. To investigate this, we have characterised copper binding to a recently discovered GnRH-type peptide from the starfish *Asterias rubens* (ArGnRH). Using a range of spectroscopic and biophysical techniques we show that this peptide can bind copper(II) and nickel(II). Copper(II) is bound in a square-planar, high-affinity (K_d ~10^{-12} M) site incorporating four nitrogen donor atoms from a histidine imidazole group, two amides and the N-terminal amine group. The ArGnRH copper affinity and geometry are quite different to GnRH-I suggesting the copper sites have evolved to suit the environment the peptides are exposed to. By comparing the copper binding sites in ArGnRH and human GnRH-I and conducting a phylogenetic analysis of GnRH-type peptide sequences from a range of species, we predict that copper-binding is an evolutionarily ancient feature of GnRH-type peptides that has been retained, modified or lost in different lineages.

Keywords: gonadotropin-releasing hormone, copper, neuropeptide, echinoderm, ATCUN motif, starfish, *Asterias rubens*

Significance to Metallomics: Gonadotropin-releasing hormone type neuropeptides are evolutionarily ancient molecules that regulate a variety of physiological processes in animals. Human gonadotropin-releasing hormone binds copper but it is not known if this is a general property of this neuropeptide family. Here we show that a starfish gonadotropin-releasing hormone type neuropeptide also binds copper and with very high affinity. Furthermore, based on phylogenetic sequence analysis we suggest that copper-binding is an ancestral feature that has evolved to suit different environmental conditions.

Introduction

Gonadotropin-releasing hormone (GnRH; pQHWSYGLRPG-NH_2) was discovered in 1971 on account of its effect in triggering release of luteinizing hormone (LH) and follicle stimulating hormone from the pituitary gland in mammals.[1] This action of GnRH is necessary for the onset of puberty and maintenance of reproductive function in adulthood.[2] Subsequently, a related neuropeptide (pQHWSHGWYPG-NH_2) was discovered in mammals and this is referred to as GnRH-II, with the prototype peptide now known as GnRH-I. Investigation of the physiological roles of GnRH-II has revealed that it is likewise involved in regulating reproductive function, but it also has non-reproductive functions.[3] GnRH-I and GnRH-II exert their effects in mammals by binding to distinct G protein-coupled receptors.[3]

Investigation of the biochemical properties of GnRH-I revealed that it binds copper via the N-terminal pQH sequence, where the metal ion is coordinated via histidine amide and imidazole nitrogens, the pyroglutamate nitrogen, and a solvent molecule.[4] Examination of the physiological relevance of copper binding to GnRH-I has revealed that copper-bound GnRH-I has a higher affinity for its receptor than non-complexed GnRH-I, resulting in enhanced release of LH from female rats.[5] This effect of copper has been linked to conformational changes that result in modification of receptor-dependent activation of downstream intracellular signalling pathways.[3] Furthermore, the conformational changes make copper-bound GnRH-I less susceptible to proteolytic degradation, which may contribute to its enhanced bioactivity *in vivo*.[6, 7] However, the affinity of GnRH-I for copper is not high enough for the complex to survive intact after transit through the hypophyseal portal circulation, and it is proposed that GnRH-I binds copper directly in the anterior pituitary near to the gonadotropin releasing cells.[8]

Analysis of the phylogenetic distribution of GnRH-related neuropeptides and their cognate G protein-coupled receptors has revealed that the evolutionary origin of this signalling system can be traced back to a common ancestor of bilaterian animals.[9, 10] For example, it has been discovered that adipokinetic hormone (AKH; pQLNFTPNWGT-NH_2) in insects and AKH-like peptides in nematodes are orthologs of vertebrate GnRH-type peptides.[11, 12] However, copper binding has thus far only been examined for mammalian GnRH-I and it is not clear if this feature is restricted to the mammalian peptide or is a feature of the broader family. Recently, a GnRH-type neuropeptide (ArGnRH; pQIHYKNPGWGPG-NH_2) and its cognate receptor (ArGnRHR) were identified in the starfish *Asterias rubens* (phylum Echinodermata) and a noteworthy feature of ArGnRH is that it has a histidine at position three.[13] Previous studies on other peptides and proteins have

revealed that the presence of a histidine residue in the third position promotes high affinity binding of copper and nickel via a (NH_2, $2N^-$, N_{im}) coordination mode in what is now termed an amino terminal copper and nickel (ATCUN) binding site.[14] The ATCUN site has been observed in many albumins and neuropeptides and we have previously identified a precursor protein in *A. rubens* which generates several ATCUN-containing neuropeptides.[15-17] In contrast to many ATCUN peptides, ArGnRH and GnRH-I have a pyroglutamate at the N-terminus and the effect of this modification on copper or nickel coordination has not been investigated. However, analysis of GnRH-I suggests that its copper affinity is several orders of magnitude lower than that of the well characterised peptide GHK which contains a histidine at position 2 and a conventional N-terminal amine.[8] Potentially, the pyroglutamate is responsible for the reduction in affinity, although other factors such as the different lengths of the peptides and the different methods used to estimate affinity must also be taken into consideration when comparing different peptides.

The objective of this study was to investigate the copper(II)- and nickel(II)-binding properties of ArGnRH and compare with the known metal-binding properties of GnRH-I. Furthermore, to gain insights into the evolution of metal binding by GnRH-type neuropeptides we investigate the phylogenetic distribution of the occurrence and position of histidine residues in the N-terminal region of GnRH-related neuropeptides.

Experimental

Asterias rubens gonadotropin-releasing hormone (ArGnRH, pQIHYKNPGWGPG-NH_2) was custom synthesised by PPR Ltd (Fareham, Hampshire, UK) at >95% purity. Synthetic GnRH-I was purchased from Auspep (Melbourne, Australia). All other chemicals were purchased from Sigma-Aldrich (Castle Hill, Sydney, Australia). The concentration of ArGnRH was determined using an extinction coefficient at 280 nm of the tryptophan (5690 $M^{-1}cm^{-1}$) and tyrosine (1280 $M^{-1}cm^{-1}$) residues. The buffer used was either 10 mM 4-ethylmorpholine (nEM) or 10 mM sodium phosphate (NaP_i). A stock (50 mM) solution of copper was prepared as $CuCl_2 \cdot 2H_2O$ in metal-free MilliQ water (18 MΩ, Millipore) and diluted to working concentrations on the day of use. Similarly, a stock (36 mM) solution of $NiCl_2$-xH_2O was prepared and diluted on the day of use.

Electronic Spectroscopy.

UV/Visible electronic spectroscopy was performed on a Cary 100 UV-Vis spectrophotometer operated with Cary WinUV software. All spectra were collected using a 1.0 cm path length cuvette over the range 200 – 800 nm at a scan rate of 300 nm/min.

Mass Spectroscopy (MS).

MS data were acquired on a XEVO-QToF (Waters Corp., Milford, MA, USA) operated in positive ion mode. The capillary voltage was 3.5 kV and spectra were collected at cone voltages of 30 V and 80 V, source temperature 80 °C and over mass ranges of 200 to 3000 Da. Spectra were collected and analysed using MassLynx software (Waters Corp., Milford, MA, USA). Peptide samples and copper complexes were prepared in water at 215 μM and diluted ×10 using a 1:1 acetonitrile:water solvent containing 0.1% formic acid. The diluted samples were applied via a direct infusion at a flow rate of 10 μL/min.

Circular Dichroism (CD) spectroscopy.

CD spectra were collected on a Jasco J810 spectrometer. Spectra were collected over the range 300 – 800 nm, with data points every 2 nm, in a 1.0 cm path length square cuvette. Routinely, 10 scans were collected and averaged. The raw signal was converted to molar ellipticity ($\Delta\varepsilon$, $M^{-1}cm^{-1}$) using the equation $\Delta\varepsilon = \theta/33000 \times c \times l$, where c = concentration (M) and l = pathlength (cm).

Nuclear Magnetic Resonance (NMR) spectroscopy.

All NMR spectra were collected on a 300 MHz Bruker Avance spectrometer equipped with a 5 mm TXI probe and operated with Topspin 3.1 software (Bruker Biospin, Germany). Proton spectra were acquired over an 11 ppm spectral width comprising 64 K complex points, and the residual water signal was suppressed using a W5 watergate sequence. Spectra were processed using SpinWorks 4.[18] Two-dimensional TOCSY spectra were acquired using a pulse program incorporating a DIPSI spin-lock sequence (80 ms) and gradient water suppression. Spectra were acquired over 11 ppm in both dimensions and processed using a $\pi/2$ shifted sine-squared window function in both directions, linear prediction to 512 real points in F1 and zero-filled to 2K real points in both dimensions.

Electron Paramagnetic Resonance (EPR) Spectroscopy.

Continuous wave EPR spectra at ~9.4 GHz (X-band) were obtained on a Bruker Elexsys E500 spectrometer operated with Bruker Xepr software and equipped with a super high-Q cavity. The microwave frequency was calibrated with an EIP548B frequency counter. A temperature of 150 ± 5K was achieved using a nitrogen gas flow-through system linked to a Eurotherm B-VT-2000 temperature controller. The power was 8 mW, the modulation amplitude was 5G, the modulation frequency was 100 kHz and the sweep time was 120 s. Spectra were simulated using the least-squares fitting algorithm in Easyspin running in Matlab R2018a.[19] The copper hyperfine and Zeeman interactions were simulated using matrix diagonalization, and after inclusion of nitrogen nuclei the nitrogen superhyperfine interactions were simulated using perturbation theory. Linewidths were fit using a correlated distribution of g- and A-values.[20]

Estimation of the ArGnRH copper dissociation constant.

The copper(II)-ArGnRH dissociation constant was estimated via a competitive metal-ion capture procedure employing glycine as the competitor.[8, 21] Individual [Cu^{II}ArGnRH] samples were prepared in nEM buffer (10 mM, pH 7.55) and glycine was titrated to a final concentration of 17.4 mM. Glycine forms a 2:1 complex with copper and this species is CD silent, therefore the spectra obtained during the titration represents only [Cu^{II}ArGnRH] and from this the fraction (θ) of Cu(II)-bound ArGnRH can be determined. When θ = 0.5, the dissociation constant, $K_d = [Cu^{2+}]_{free}$ and $[Cu^{2+}]_{free,}$ in the presence of glycine, is given by[21]:

$$[Cu^{2+}]_{free} = 1/(1 + K_{a1}[gly] + K_{a1}K_{a2}[gly]^2) \cdot ([Cu^{2+}]_{total} - [Cu^{II}ArGnRH]) \quad (1)$$

The stepwise dissociation constants ($K_d = 1/K_a$) for [$Cu^{II}(gly)_2$] at pH 7.55 are 0.89 μM (K_{d1}) and 8.91 μM (K_{d2}) [22]. The affinity determined in this manner should be considered a maximum as previously described.[23]

Investigation of the phylogenetic distribution of GnRH-type neuropeptides that have a histidine residue at position three

To assess the evolutionary origin of the occurrence of a histidine residue at position three in ArGnRH, the sequences of neuropeptides that have been identified as ligands for GnRH-type receptors were assembled by surveying published literature in this field of research, which has been reviewed recently.[10] The sequences of the peptides were then aligned manually and ordered in accordance with the known phylogenetic relationships of the taxa from which the peptides are derived.[24, 25] In this way, it was possible to examine the

phylogenetic distribution GnRH-type neuropeptides with a histidine residue at position three and thereby investigate the evolutionary origin(s) of this characteristic.

Results and Discussion

ArGnRH binds copper in a high affinity, square planar complex.

To assess the copper-binding ability of ArGnRH we first used electronic spectroscopy. The addition of Cu(II) to a solution of ArGnRH results in the appearance of a peak in the absorption spectrum at 530 nm (Figure 1A). With continued addition of copper, the absorption rises, but the slope of the binding curve changes beyond one equivalent Cu^{2+} (Figure 1A (*inset*)), suggesting a stoichiometry of 1:1. The peak at 530 nm is due to *d-d* transitions of the Cu^{2+} ion. The peak at 530 nm is different to that observed for Cu(II) binding to GnRH-I, which occurs near 590 nm (Figure 1A, dashed line).[4, 8] The shift to higher energy for [Cu^{II}ArGnRH] compared to [Cu^{II}GnRH-I] suggests that ArGnRH has stronger-field ligands than GnRH-I, most likely due to the inclusion of more N-donors in the complex at the expense of weaker O-donors. We next confirmed the 1:1 stoichiometry using mass spectrometry. The electrospray mass spectra of apo-ArGnRH and copper-bound peptide are shown in Fig. 1B. The spectrum of apo-ArGnRH shows predominant peaks at *m/z* 1335.59 and m/z 1358.6 corresponding to ArGnRH and its sodium adduct, respectively. Addition of an equimolar amount of Cu^{2+} results in the spectrum in Fig. 1B(b). This spectrum has the same peaks corresponding to apo-ArGnRH, but also peaks corresponding to [Cu^{II}ArGnRH – 3H]$^+$ (*m/z* 1396.5) and the sodium adduct of the copper complex (*m/z* 1418.9). We next analysed a sample containing a ×10 molar ratio of Cu(II). The mass spectrum of this sample (Fig. 1B(c)) shows a high proportion of the [Cu^{II}ArGnRH – 3H]$^+$ and its sodium adduct. At this high concentration of copper a small peak corresponding to dinuclear metal complex is apparent at *m/z* 1457.5. Spurious binding of an additional copper atom may account for the lack of a distinct plateau in the UV/Vis titration data beyond one equivalent copper (Fig. 1A inset). Taken together with the electronic spectroscopy results, the MS data suggests that the most stable complex is [Cu^{II}ArGnRH]. We predict that the loss of three protons to form the complex at *m/z* 1396.5 is due to loss of amide protons driven by the copper binding.

To determine the ligands contributing to the coordination environment in [Cu^{II}ArGnRH] we used EPR spectroscopy. The experimental EPR spectrum of a frozen solution of [Cu^{II}ArGnRH] (Figure 1C, exp) shows a typical axial-type spectrum copper complex (g_x, $g_y < g_z$). Mapping the g_z and A_z values to the plots developed by Peisach and Blumberg suggests the copper in [Cu^{II}ArGnRH] is coordinated to 4N or 3N1O ligands.[26] The

involvement of nitrogen ligands is evident because the perpendicular region ($g_{x/y}$, 320-340 mT) of the experimental spectrum contains peaks due to coupling of the unpaired electron on copper to the nuclear magnetic moment of coordinated nitrogen atoms (superhyperfine (shf) coupling). The number of shf peaks is correlated to the number of coordinated nitrogen atoms and these are more easily observed in the second differential spectrum (Fig. 1C, inset). In an ideal complex the number of coordinated nitrogen atoms (n) is related to the number of shf peaks by 2n+1, so four N ligands gives rise to nine shf peaks. In Fig. 1C, [Cu^{II}ArGnRH] has more than nine peaks in the $g_{x,y}$ region. The $g_{x,y}$ region can be complicated by the presence of more than one species as well as distortion away from ideal symmetry. The low value of A_z for [Cu^{II}ArGnRH) can be associated with rhombic distortion and therefore the spectrum in Fig. 1C (and inset) was simulated assuming a distorted complex (i.e. $g_x \neq g_y \neq g_z$) with four magnetically equivalent nitrogen donor atoms using the spin Hamiltonian parameters given in table 1. The simulated spectrum shows very good agreement with the experimental spectrum (Fig. 1C), which confirms the presence of four coordinating nitrogen atoms. However, although the number and position of the superhyperfine coupling peaks are well simulated, the intensity of the lines is not accurate, which may indicate the presence of a small amount of a 3N1O complex as suggested by the Peisach-Blumberg analysis.[27]

To determine the identity of the nitrogen donors we first used NMR. The presence of paramagnetic Cu(II) causes line-broadening of atoms within about 7 Å of the copper centre. In the ^{1}H NMR spectra of [Cu^{II}ArGnRH] acquired prior to the addition of copper (Figure 2A, apo) and after the addition of low concentrations of copper (Figure 2A, 0.08 and 0.24 eq. Cu(II)) we see significant broadening of peaks arising from protons on the histidine imidazole group (C_2H and C_4H). The presence of 0.24 eq. copper has effectively broadened these peaks beyond detection. Other peaks that show broadening and a loss of intensity are those near 2.85 ppm (Figure 2A), attributable to the histidine Hβ protons, and peaks near 1.7 ppm. The peaks at 1.7 ppm are difficult to identify given an overlap of several different protons, however this region does contain contributions from pyroglutamate protons. In general there is a minor broadening of all of the peaks in the spectrum, presumably due to the small size of the peptide where all protons are relatively near the metal centre. The nitrogen ligands were also identified using CD spectroscopy. The CD spectrum of [Cu^{II}ArGnRH] (Figure 2B, solid line) shows negative peaks at 325 and 575 nm, and a positive peak at 490 nm. The presence of peaks in the visible region is due to chirality in the metal binding site and is usually associated with binding to main-chain amide nitrogen atoms.[28] CD peaks near

325 nm can be attributed to $N_{Im} \rightarrow Cu(II)$ transitions suggesting, in accord with the NMR data, copper coordination to the histidine imidazole nitrogen atom. Previous analysis of copper complexes by CD spectroscopy has highlighted how the appearance of the visible peaks correlates with structure.[29] The positive band at 460 nm and weaker negative band at 575 nm is similar to the spectrum of H_2N-xxH tripeptides in which the metal is coordinated to histidine, the amino terminal N and amide nitrogens and where the His imidazole group is located below the plane of the backbone atoms.[29] ArGnRH has the N-terminal sequence pQIH so it is not unreasonable that it should adopt similar copper complexes to simple tripeptides. In general, the effect of a N-terminal pyroglutamate on copper coordination has not been investigated, but even though ArGnRH has a pyroglutamate it appears that it forms a copper complex having the same, or very similar, geometry as a peptide with a free N-terminal amine. Additionally, pyroglutamate as the first amino-acid is similar to having proline in position 1 which has previously been shown to not modify oligopeptide metal binding.[30] Although the CD spectra of [Cu^{II}ArGnRH] and [Cu^{II}GnRH-I] (Figure 2B, dashed line) both highlight the inclusion of imidazole coordination, there is significant difference in the visible region, which is consistent with [Cu^{II}GnRH-I] adopting a 3N1O copper complex, but [Cu^{II}ArGnRH] having a 4N environment.

Peptides and proteins that contain copper-binding H_2N-xxH sequences (termed ATCUN motifs) can have high affinity binding.[31] In mammalian biology, nanomolar copper dissociation constants are considered physiologically relevant. However, in marine animals like starfish this will not be the case because the copper concentration in seawater is low (10^{-8} M) and the presence of high-affinity chelating compounds means that the free copper concentration is very low (10^{-11} -10^{-12} M).[32] The ionic composition of starfish body fluids is similar to that of seawater and therefore proteins having only a nanomolar dissociation constant are unlikely to be metallated to any extent. To assess the affinity of ArGnRH for copper we used a competitive metal-ion capture technique employing the amino acid glycine as a competitor. Glycine was titrated into a solution of [Cu^{II}ArGnRH] and CD was used to monitor the abstraction of copper from the complex. The loss of intensity of the CD peaks (Figure 2C) correlates with the binding of copper by glycine to form non-chiral [$Cu(gly)_2$]. The concentration of glycine required to abstract half the copper from [Cu^{II}ArGnRH] (θ = 0.5) was estimated based on the concentration of glycine required to reduce the intensity of the CD band at 490 nm to half its original value which was estimated as being 10.8 mM (Figure 2C, dashed line) corresponding to a [gly]:[ArGnRH] ratio of ~73:1. Using an

identical method we previously established that mammalian GnRH-I lost 50% of bound copper at a [gly]:[GnRH-I] ratio of ~ 3:1, suggesting that ArGnRH has a copper affinity much higher than mammalian GnRH-I.[8] Indeed, using eq. 1 we estimate a dissociation constant of ~ 5.2×10^{-12} M which is several orders of magnitude lower than mammalian GnRH-I (~0.9×10^{-9} M). However, unlike the loss of copper from GnRH-I,[8] the abstraction of copper from ArGnRH by glycine was not linear over the entire glycine concentration range, which may be due to various reasons including peptide structural changes or formation of ternary complexes. Further analysis of the underlying reasons for the non-linear abstraction of copper was not undertaken and therefore the dissociation constant must be considered an estimate. Nevertheless, the result is entirely consistent with the different binding sites, GnRH-I has a histidine in position 2 (pQH…) whereas ArGnRH has a histidine in position 3 (pQIH…), and a dissociation of this magnitude is in a similar range to other proteins and peptides having a H_2N-xxH copper-binding sequence.[31]

ArGnRH binds Ni(II) forming a 5-coordinate, diamagnetic complex.

The binding of copper by peptides and proteins having an ATCUN motif (histidine at position 3) is often mimicked by Ni(II) binding. The copper experiments indicate that the N-terminal pyroglutamate does not impede the copper coordination, suggesting that Ni(II) should also bind. Although both Cu(II) and Ni(II) can promote deprotonation of amide nitrogens, Ni(II) generally requires higher pHs to do so.[30] To investigate metal binding we first titrated Ni(II) into pH 7.2 and pH 9.3 solutions of ArGnRH and followed the binding by electronic spectroscopy. The spectra show that at pH 7.2 there is little evidence of binding either in the UV or the visible regions of the spectrum (Figure 3, the peak at 280 nm is due to $n/\pi \rightarrow \pi^*$ transitions of aromatic amino acids). In contrast, increasing the pH to 9.3 results in the formation of a peak near 260 nm as well as in the region between 400 and 500 nm. The intensity and wavelength of the peak near 260 nm is indicative of a ligand-to-metal charge transfer transition (note that the high absorption makes analysis inaccurate).[33] The weak peaks at 410 and 490 nm are d-d transitions and peaks in this area are usually due to diamagnetic complexes. We have observed similar peaks upon the addition of Ni(II) to *A. rubens* SALMFamide-type neuropeptides, but we observed only the presence of a single absorption band near 420 nm.[17] A single band is often attributed to a diamagnetic square-planar complex, but Ni(II) can also adopt a five-coordinate, square pyramidal geometry that has C_{4v} symmetry and is a low-spin, diamagnetic complex.[33] These complexes have more

than one peak in the visible region and we predict that the two peaks at 410 and 490 nm indicate that Ni(II) in [Ni^{II}ArGnRH] is in a 5-coordinate geometry. Indeed, we observed two peaks in the same region of the electronic spectrum of Ni(II) bound to peptides derived from the prion protein, which was subsequently shown to correspond to a coupled, 5-coordinate Ni(II).[34, 35]

The diamagnetic nature of the complex means that NMR can be used to help identify coordinating ligands. The aromatic/amide region of the NMR spectrum of apo-ArGnRH is shown in Figure 4A (lowest trace), and the assignment of the peaks is highlighted. At the high pH of this experiment (pH ~ 9.2) the amide protons are not observed due to exchange with the buffer. The addition of Ni(II) causes clearly observable changes to this region of the spectrum, with peaks due to His imidazole protons (C_4H and C_2H) and the Tyr aromatic side chain (H2,6 and H3,5) in the apo peptide decreasing in intensity and a whole new set appearing (e.g. at 6.59 ppm and 6.83 ppm for His3 imidazole protons). The appearance of a Ni(II)-bound set along with the apo peaks indicates that the on-off rate of Ni(II) is slow compared to the NMR timescale. At approximately 0.4 eq. Ni(II) there is almost equal intensity of peaks due to apo and Ni(II)-bound ArGnRH, and there is no evidence of peaks due to apo-ArGnRH once one equivalent has been reached. This is consistent with a UV/Vis titration (data not shown) and indicates a binding stoichiometry of 1:1. The assignment of peaks that have moved upon Ni(II) binding are shown in Figure 4A (top trace) suggesting that both His3 and Tyr 4 are involved in coordination. The lack of any changes to side chain protons of Asn5 and Trp9 supports the idea that Ni(II) binding is occurring at the N-terminal region. Analysis of the aliphatic region shows that there are chemical shift changes to many peaks; notably the side-chain methyl groups of Ile2 have moved in the Ni(II)-bound peptide (Figure 4B). The γ-CH_3 doublet has moved 0.364 ppm downfield upon Ni(II) binding, and the ε-CH_3 triplet has moved 0.106 ppm downfield. In this case, the downfield shifts indicate a deshielding effect due to magnetic anisotropic effects of an aromatic group, which is most likely due to movement of the tyrosine and not the tryptophan. The γ-CH_3 group is relatively more effected and the deshielding suggests it is located near the plane of the aromatic ring. Previously, mammalian GnRH-I was predicted to bind Ni(II) via the same ligands it binds copper (N-terminal pyroglutamate nitrogen, an amide and the His2 imidazole nitrogen) and it is likely that ArGnRH uses similar ligands as its basis for binding Ni(II).[4] The requirement for high pH values to promote binding suggests amide coordination, and, with changes to the His imidazole proton chemical shifts, we suggest that the binding site is comprised of the N-

terminal pQ nitrogen, the amides of Ile2 and His3 and a His3 imidazole nitrogen similar to conventional ATCUN sites. It is highly unlikely that the chemical shift changes of the Tyr aromatic protons are due to coordination to the Tyr amide nitrogen, rather, and in contrast to GnRH-I, we predict that the tyrosine changes are due to coordination of Ni(II) to the hydroxyl oxygen, which may displace the hydroxyl proton. Indeed, and not unexpectedly, there are substantial chemical shift changes to Tyr aromatic protons after deprotonation (pKa = 10.1). We predict that Ni(II) is coordinated with a $\{NH_2, 2N^-, N_{im}, O_{Tyr}\}$ donor set, and if the tyrosine oxygen is coordinated in the apical position, i.e. sits above the plane of the nitrogen ligands, then a structure can be achieved where the Ile methyl groups are located in the plane of the aromatic ring. A schematic diagram of the copper and nickel ArGnRH complexes consistent with the experimental evidence is shown in Figure 5.

The phylogenetic distribution and evolutionary origin(s) of N-terminal histidines in GnRH-type neuropeptides

Investigation of the occurrence of a histidine residue at the third position in GnRH-type neuropeptides revealed that it is not unique to *A. rubens*, but it is also a feature of other echinoderms, including other starfish species,[36] brittle stars,[37] and sea urchins[38] (Figure 6). However, GnRH-type neuropeptides that have been identified in other invertebrate deuterostomes do not have this feature. Thus, GnRH-type neuropeptides in the urochordate *Ciona intestinalis* have a histidine in position two, in common with GnRH-type neuropeptides in humans and other vertebrates (Figure 6). What about in the other branch of the Bilateria – the protostomes? It appears that histidine residues are typically not present in the GnRH-type neuropeptides of protostomes. Thus, GnRH-type neuropeptides in the nematode *C. elegans* and the annelid *Platynereis dumerilli* do not have histidine residues. Likewise, the paralogous AKH/RCPH-type and ACP-type GnRH-related neuropeptides of arthropods also do not contain histidine residues. Interestingly, however, GnRH-type neuropeptides in molluscs have a histidine residue in the third position, as exemplified by the *Aplysia californica* GnRH-type neuropeptide shown in Figure 6.[10, 39] Interestingly, the N-terminal sequence of *A. californica* GnRH (AcGnRH) is very similar to ArGnRH, with the first three residues being identical (pGlu-Ile-His) and the fourth residue structurally similar (Tyr/Phe). Therefore, the biophysical properties of AcGnRH with respect to copper binding are likely to be very similar to those reported here for ArGnRH.

What is the significance of the occurrence of GnRH-type peptides with a histidine at the third position in both echinoderms and molluscs? One possible explanation is that this is a feature that has evolved independently in both phyla. Alternatively, because this feature occurs in both the deuterostome branch (echinoderms) and protostome branch (molluscs) of the Bilateria, it may have been a characteristic of the GnRH-type neuropeptide present in the common ancestor of protostomes and deuterostomes, but with subsequent loss in multiple lineages. An argument in favour of the latter scenario is the occurrence of a histidine residue at position two in the GnRH-type neuropeptides of chordates, which could be explained by a mutation-induced loss of a codon in the position between the N-terminal glutamine-encoding codon and the histidine-encoding codon in the GnRH gene of a common ancestor of the chordates. Further evidence that the presence of a histidine residue in the N-terminal region of GnRH-type neuropeptides, although not necessarily at position three, can be found from analysis of the sequences of corazonin-type neuropeptides, which are paralogs of GnRH-type neuropeptides. Corazonin itself (pQTFQYSRGWTN-NH_2), which was first discovered in insects, does not contain a histidine residue. However, orthologs of corazonin that have been discovered in echinoderms, hemichordates and molluscs contain a histidine residue in their N-terminal region. For example, a corazonin-type neuropeptide in i). the starfish *A. rubens* has the sequence HNTFTMGGQNRWKAG-NH_2, ii). the hemichordate *S. kowalevskii* has the sequence pQPHFSLKDRYRWKP-NH_2 and iii). the mollusc *A. californica* has the sequence pQNYHFSNGWYA-NH_2.[10, 13] The gene duplication event that gave rise to the paralogous GnRH-type and corazonin-type neuropeptides probably occurred in a common ancestor of the Bilateria.[10, 13] Therefore, the occurrence of histidine residues in the N-terminal region of at least some GnRH-type and some corazonin-type neuropeptides suggests that this was probably a feature of the common ancestral neuropeptide, which has then been variously retained or lost in representatives of both of the descendent neuropeptide families.

What is the functional significance of a high-affinity copper- and nickel-binding site in ArGnRH and other GnRH-type neuropeptides?

Recent investigation of the functional consequences of copper coordination to mammalian GnRH-I has revealed that the complex modifies receptor-mediated activation of downstream intracellular signalling pathways compared to apo-GnRH-I.[7] This activity is complemented by the ability of the copper-complex to resist degradation by extracellular peptidases and it is not unreasonable to speculate that copper-bound ArGnRH will have similar properties.[6] In ArGnRH, the ATCUN-motif drives high-affinity copper binding and

we can predict that the complex will also have reasonably high stability. Recent work by Miyamoto *et al*. has shown that the presence of hydrophobic, bulky amino acids at position 1 and 2 of the ATCUN motif is key to enhanced stability.[40] ArGnRH has the N-terminal sequence pQIH and the isoleucine is likely to support high stability, due in part to sterically hindering access of competitors to the metal centre.[40] Indeed, the ability of [Cu^{II}ArGnRH] to survive the sample conditions (acidic conditions) and the ionisation process during ESI-MS (Fig.1B) supports high stability. The difference in copper affinity between mammalian GnRH-I and ArGnRH may reflect the chemical composition of the milieu into which they are released physiologically. Thus, GnRH-I does not need a very high affinity because, once out of the hypophyseal portal circulation, it can likely obtain copper from the relatively copper-rich anterior pituitary. In contrast, because the extracellular milieu in starfish has a similar ionic composition to seawater, ArGnRH probably competes with other high-affinity components to obtain and retain copper in a copper-depleted internal environment.[41] The role of Ni(II) in ArGnRH function may be similar to that of copper. Ni(II) in coastal seawater can reach 5 μg/L as a mix of aqueous Ni^{2+} and as complexes with inorganic ligands, e.g. as $NiCO_3$.[42] Given the changes that Ni(II) induces in the structure of ArGnRH in order to form [Ni^{II}ArGnRH] (Fig. 4) we predict that Ni(II)-binding may alter receptor activation compared to ArGnRH. The recent identification of the receptor for ArGnRH now allows these predictions to be experimentally tested.[13] How the Cu(II)- and Ni(II)-binding to ArGnRH compares and relates to GnRH-type peptides in other species remains to be determined. Notably, some peptides contain more than one histidine, including mammalian GnRH-II (Figure 6), but the impact on copper and nickel affinity, stability and peptide function has not been investigated for these peptides.

Conclusion

In this work we have characterised copper and nickel binding to the recently identified GnRH-type neuropeptide from the starfish *A. rubens*. To the best of our knowledge, this work is the first investigation of copper and nickel binding to a GnRH-type neuropeptide from a non-mammalian species. The copper binding characteristics of ArGnRH are entirely consistent with the presence of an ATCUN motif, and five-coordinate nickel binding is not unprecedented in this motif.[14] Unlike mammalian GnRH-I, the presence of both copper and nickel in seawater suggests that both metals may be relevant for ArGnRH function. Furthermore, the occurrence of an N-terminally located histidine residue in GnRH-

related neuropeptides from a variety of phyla suggests that copper-binding in this family of neuropeptides is an evolutionarily ancient property that can be traced back to the common ancestor of the Bilateria, but with subsequent loss in some lineages (e.g. in insect AKH-type neuropeptides).

Acknowledgements

Assoc. Prof. Jeffrey Harmer from the Centre for Advanced Imaging, The University of Queensland, is thanked for assistance with operating the EPR spectrometer. Synthesis of ArGnRH was funded by a grant awarded to MRE by the BBSRC (BB/M001644/1).

References

1. H. Matsuo, Y. Baba, R. M. Nair, A. Arimura and A. V. Schally, Structure of the porcine LH- and FSH-releasing hormone. I. The proposed amino acid sequence, *Biochem Biophys Res Commun*, 1971, **43**, 1334-1339.
2. G. Fink, in *Neuroendocrinology in Physiology and Medicine*, eds. P. M. Conn and M. E. Freeman, Humana Press, Totowa, NJ., 2000.
3. R. P. Millar, Z. L. Lu, A. J. Pawson, C. A. Flanagan, K. Morgan and S. R. Maudsley, Gonadotropin-releasing hormone receptors, *Endocr Rev*, 2004, **25**, 235-275.
4. K. Nakamura, M. Kodaka, I. M. El-Mehasseb, A. Gajewska, H. Okuno, E. Ochwanowska, B. Witek, H. Kozlowski and K. Kochman, Further structural analysis of GnRH complexes with metal ions, *Neuro Endocrinol Lett*, 2005, **26**, 247-252.
5. K. Kochman, A. Gajewska, H. Kozlowski, E. Masiukiewicz and B. Rzeszotarska, Increased LH and FSH release from the anterior pituitary of ovariectomized rat, in vivo, by copper-, nickel-, and zinc-LHRH complexes, *J Inorg Biochem*, 1992, **48**, 41-46.
6. A. Herman, H. Kozlowski, M. Czauderna, K. Kochman, K. Kulon and A. Gajewska, Gonadoliberin (GnRH) and its copper complex (Cu-GnRH) enzymatic degradation in hypothalamic and pituitary tissue in vitro, *J Physiol Pharmacol*, 2012, **63**, 69-75.
7. A. Gajewska, M. Zielinska-Gorska, E. Wolinska-Witort, G. Siawrys, M. Baran, G. Kotarba and K. Biernacka, Intracellular mechanisms involved in copper-gonadotropin-releasing hormone (Cu-GnRH) complex-induced cAMP/PKA signaling in female rat anterior pituitary cells in vitro, *Brain Res Bull*, 2016, **120**, 75-82.
8. A. S. Gul, K. K. Tran and C. E. Jones, Neurokinin B and serum albumin limit copper binding to mammalian gonadotropin releasing hormone, *Biochem Biophys Res Commun*, 2018, **497**, 1-6.
9. G. J. Roch, E. R. Busby and N. M. Sherwood, GnRH receptors and peptides: skating backward, *Gen Comp Endocrinol*, 2014, **209**, 118-134.
10. M. Zandawala, S. Tian and M. R. Elphick, The evolution and nomenclature of GnRH-type and corazonin-type neuropeptide signaling systems, *Gen Comp Endocrinol*, 2018, **264**, 64-77.
11. F. Staubli, T. J. Jorgensen, G. Cazzamali, M. Williamson, C. Lenz, L. Sondergaard, P. Roepstorff and C. J. Grimmelikhuijzen, Molecular identification of the insect adipokinetic hormone receptors, *Proc Natl Acad Sci U S A*, 2002, **99**, 3446-3451.
12. M. Lindemans, F. Liu, T. Janssen, S. J. Husson, I. Mertens, G. Gade and L. Schoofs, Adipokinetic hormone signaling through the gonadotropin-releasing hormone

receptor modulates egg-laying in Caenorhabditis elegans, *Proc Natl Acad Sci U S A*, 2009, **106**, 1642-1647.
13. S. Tian, M. Zandawala, I. Beets, E. Baytemur, S. E. Slade, J. H. Scrivens and M. R. Elphick, Urbilaterian origin of paralogous GnRH and corazonin neuropeptide signalling pathways, *Sci Rep*, 2016, **6**, 28788.
14. C. Harford and B. Sarkar, Amino terminal Cu(II)- and Ni(II)-binding (ATCUN) motif of proteins and peptides: Metal binding, DNA cleavage, and other properties., *Acc. Chem. Res.*, 1997, **30**, 123-130.
15. C. Harford and B. Sarkar, Neuromedin C binds Cu(II) and Ni(II) via the ATCUN motif: implications for the CNS and cancer growth, *Biochem Biophys Res Commun*, 1995, **209**, 877-882.
16. D. Russino, E. McDonald, L. Hejazi, G. R. Hanson and C. E. Jones, The Tachykinin Peptide Neurokinin B Binds Copper Forming an Unusual [CuII(NKB)] Complex and Inhibits Copper Uptake into 1321N1 Astrocytoma Cells, *ACS Chem Neurosci*, 2013, **4**, 1371-1381.
17. C. E. Jones, M. Zandawala, D. C. Semmens, S. Anderson, G. R. Hanson, D. A. Janies and M. R. Elphick, Identification of a neuropeptide precursor protein that gives rise to a "cocktail" of peptides that bind Cu(II) and generate metal-linked dimers, *Biochim Biophys Acta*, 2016, **1860**, 57-66.
18. K. Marat, Spinworks 4.2.0, 2015, University of Manitoba.
19. S. Stoll and A. Schweiger, EasySpin, a comprehensive software package for spectral simulation and analysis in EPR, *J Magn Reson*, 2006, **178**, 42-55.
20. W. Froncisz and J. S. Hyde, Broadening by Strains of Lines in the G-Parallel Region of Cu2+ Electron-Paramagnetic-Resonance spectra., *J Chem Phys*, 1980, **73**, 3123-3131.
21. C. J. Sarell, C. D. Syme, S. E. Rigby and J. H. Viles, Copper(II) binding to amyloid-beta fibrils of Alzheimer's disease reveals a picomolar affinity: stoichiometry and coordination geometry are independent of Abeta oligomeric form, *Biochemistry*, 2009, **48**, 4388-4402.
22. R. M. C. Dawson, D. C. Elliot, W. H. Elliot and K. M. Jones, *Data for Biochemical Research*, Oxford University Press, Oxford, 3rd edn., 1986.
23. A. R. Thompsett, S. R. Abdelraheim, M. Daniels and D. R. Brown, High affinity binding between copper and full-length prion protein identified by two different techniques, *J Biol Chem*, 2005, **280**, 42750-42758.
24. P. W. H. Holland, *The Animal Kingdom: A Very Short Introduction.*, Oxford University Press, Oxford; New York, 2011.
25. M. J. Telford, G. E. Budd and H. Philippe, Phylogenomic Insights into Animal Evolution, *Curr Biol*, 2015, **25**, R876-887.
26. J. Peisach and W. E. Blumberg, Structural implications derived from the analysis of electron paramagnetic resonance spectra of natural and artificial copper proteins, *Arch Biochem Biophys*, 1974, **165**, 691-708.
27. J. S. Hyde, B. Bennett, E. D. Walter, G. L. Millhauser, J. W. Sidabras and W. E. Antholine, EPR of Cu2+ prion protein constructs at 2 GHz using the g(perpendicular) region to characterize nitrogen ligation, *Biophys J*, 2009, **96**, 3354-3362.
28. J. M. Tsangaris and R. B. Martin, Visible circular dichroism of copper(II) complexes of amino acids and peptides, *J Am Chem Soc*, 1970, **92**, 4255-4260.
29. H. F. Stanyon, X. Cong, Y. Chen, N. Shahidullah, G. Rossetti, J. Dreyer, G. Papamokos, P. Carloni and J. H. Viles, Developing predictive rules for coordination geometry from visible circular dichroism of copper(II) and nickel(II) ions in histidine and amide main-chain complexes, *FEBS J*, 2014, **281**, 3945-3954.

30. H. Kozlowski, W. Bal, M. Dyba and T. Kowalik-Jankowska, Specific structure-stability relations in metallopeptides, *Coord Chem Rev*, 1999, **184**, 319-346.
31. A. Trapaidze, C. Hureau, W. Bal, M. Winterhalter and P. Faller, Thermodynamic study of Cu2+ binding to the DAHK and GHK peptides by isothermal titration calorimetry (ITC) with the weaker competitor glycine, *J Biol Inorg Chem*, 2012, **17**, 37-47.
32. M. B. Kogut and B. M. Voelker, Strong copper-binding behavior of terrestrial humic substances in seawater, *Environ Sci Technol*, 2001, **35**, 1149-1156.
33. A. B. P. Lever, *Inorganic Electronic Spectroscopy*, Elsevier Science Publishers, Amsterdam, 1986.
34. C. E. Jones, M. Klewpatinond, S. R. Abdelraheim, D. R. Brown and J. H. Viles, Probing copper^{2+} binding to the prion protein-using diamagnetic nickel^{2+} and ^{1}H NMR: The unstructured N terminus facilitates the coordination of six copper^{2+} ions at physiological concentrations, *J Mol Biol*, 2005, **346**, 1393-1407.
35. J. Shearer and P. Soh, Ni K-edge XAS suggests that coordination of Ni(II) to the unstructured amyloidogenic region of the human prion protein produces a Ni(2) bis-mu-hydroxo dimer, *J Inorg Biochem*, 2007, **101**, 370-373.
36. M. K. Smith, T. Wang, S. Suwansa-Ard, C. A. Motti, A. Elizur, M. Zhao, M. L. Rowe, M. R. Hall, M. R. Elphick and S. F. Cummins, The neuropeptidome of the Crown-of-Thorns Starfish, Acanthaster planci, *J Proteomics*, 2017, **165**, 61-68.
37. M. Zandawala, I. Moghul, L. A. Yanez Guerra, J. Delroisse, N. Abylkassimova, A. F. Hugall, T. D. O'Hara and M. R. Elphick, Discovery of novel representatives of bilaterian neuropeptide families and reconstruction of neuropeptide precursor evolution in ophiuroid echinoderms, *Open Biol*, 2017, **7**.
38. M. L. Rowe and M. R. Elphick, The neuropeptide transcriptome of a model echinoderm, the sea urchin Strongylocentrotus purpuratus, *Gen Comp Endocrinol*, 2012, **179**, 331-344.
39. J. I. Johnson, S. I. Kavanaugh, C. Nguyen and P. S. Tsai, Localization and functional characterization of a novel adipokinetic hormone in the mollusk, Aplysia californica, *PLoS One*, 2014, **9**, e106014.
40. T. Miyamoto, Y. Fukino, S. Kamino, M. Ueda and S. Enomoto, Enhanced stability of Cu(2+)-ATCUN complexes under physiologically relevant conditions by insertion of structurally bulky and hydrophobic amino acid residues into the ATCUN motif, *Dalton Trans*, 2016, **45**, 9436-9445.
41. J. Binyon, Ionic Regulation and Mode of Adjustment to Reduced Salinity of Starfish Asterias Rubens L, *J Mar Biol Assoc Uk*, 1962, **42**, 49-64.
42. A. N. Bautista-Flores, E. R. De San Miguel, J. d. Gyves and J. A. Jonsson, Nickel (II) Preconcentration and Speciation Analysis During Transport from Aqueous Solutions Using a Hollow-fiber Permeation Liquid Membrane (HFPLM) Device, *Membranes (Basel)*, 2011, **1**, 217-231.

Figure legends.

Figure 1. ArGnRH binds one equivalent of Cu(II) in a four-nitrogen environment. (A) Titration of ArGnRH (121.5 μM, 10mM nEM, pH 7.3) with Cu^{2+} results in an absorption peak at 530 nm (black, solid line). The slope of the binding curve changes at one equivalent of added copper, suggesting a 1:1 stoichiometry (*inset*). The maximal absorption wavelength at 530 nm is blue-shifted compared to mammalian GnRH1 (red, dotted line) which has a maximal absorption near 590 nm. (B) Mass spectra of (a) apo-ArGnRH, (b) [Cu^{II}ArGnRH] and (c) ArGnRH in the presence of excess (×10 molar equivalents) Cu(II). All samples are 21.5 μM ArGnRH. (C) First derivative experimental EPR spectrum of copper-bound ArGnRH (350 μM, 10mM nEM, pH 7.4)(black solid line, exp.) shows features typical for axially coordinated Cu^{2+}. The experimental spectrum can be well simulated (red dotted line, sim.) assuming the metal has four nitrogen donor groups and with spin Hamiltonian parameters given in table 1. The second derivative expanded at $g_{x/y}$ (*inset*) highlights the presence of nitrogen coupling (black solid line is experiment, red dotted line is simulation).

Figure 2. ArGnRH uses His3 to bind copper(II) with high affinity. (A) Titration of ArGnRH (316 μM, 10mM NaP_i, pH 7.4) with Cu^{2+} results in broadening and loss of peaks due to histidine imidiazole C_2 and C_4 protons (arrowed at 6.75 and 7.6 ppm). Peaks at 2.8 ppm (expanded right) also show broadening and can be attributed to histidine Hβ protons. (B) The CD spectrum of [Cu^{II}ArGnRH] (black solid line) is similar to mammalian [Cu^{II}GnRH1] (red dotted line) between 200 and 300 nm but is different in the visible region. The difference is consistent with different donor groups and geometries in the two complexes. (C) Titration of [Cu^{II}ArGnRH] (148.5 μM, 10 mM nEM, pH7.4) with glycine shows that a high glycine concentration is required to abstract Cu^{2+} from [Cu^{II}ArGnRH]. The dashed line represents the glycine concentration at which [Cu^{II}ArGnRH] has lost 50% copper. The affinity of ArGnRH for copper can be estimated as described in the text.

Figure 3. ArGnRH binds Ni(II). The addition of Ni(II) to apo-ArGnRH (293.5 μM, 10 mM nEM) results in the formation of a complex at pH 9.3 but not at pH 7.2. At pH 9.3, the presence of an absorption at ~250 nm can be attributed to a ligand-to-metal-charge transfer transition, whilst the two peaks between 400 and 500 nm can be attributed to d-d transitions in a five-coordinate, square-pyramidal diamagnetic complex.[33]

Figure 4. NMR analysis of Ni(II) binding to ArGnRH. (A) The titration of Ni(II) into ArGnRH (500 μM, 10mM nEM, 10% D_2O, pH 9.3) results in a change in the aromatic region of the NMR spectrum (6.5– 7.6 ppm). Peaks due to Asn5 and Trp9 are not affected, but all others in the apo-spectrum (lowest trace) are progressively lost and a new set become apparent. At one equivalent of Ni(II) only the new set of peaks are apparent. The shifted protons are the histidine imidazole C2 and C4 protons, and the tyrosine C2,6 and C3,5 aromatic ring protons. In the aliphatic region (B) a notable shift of peaks as occurred to the methyl protons of Ile2 (arrowed), although shifts are noticeable throughout the spectrum. Note that spectra in the aliphatic region were acquired on ArGnRH in H_2O/10%D_2O, pH9.3 due to the unavailability of deuterated nEM.

Figure 5. Schematic of the ArGnRH copper and nickel sites. (A) ArGnRH binds Cu^{2+} in a square-planar, four-nitrogen site and (B) Ni^{2+} in a five-coordinate square-pyramidal site with the tyrosine phenolate oxygen the apical donor group.

Figure 6. Phylogenetic diagram showing the occurrence of histidine residues in GnRH-type neuropeptides from different taxa. Bilaterian animals comprise two clades, the deuterostomes (e.g. Chordates and Echinoderms) and protostomes (e.g. molluscs, annelids, nematodes and arthropods). The positions of histidine residues (red) in the N-terminal region of peptides are shown. Peptides that have a histidine in the third position (shaded in grey) include the *Asterias rubens* GnRH-type peptide (ArGnRH), which has been shown in this study to have a high-affinity copper binding site, and a peptide in the mollusc *Aplysia californica* (A cal), which is predicted to also have a high-affinity copper binding site. Because the occurrence of a histidine residue at position three is a feature of both a deuterostomian phylum (echinoderms) and a protostomain phylum (molluscs), this may be an evolutionarily ancient characteristic that can be traced to the common ancestor of the Bilateria but with subsequent positional modification or loss in other lineages. Sequence abbrevations: pQ = N-terminal pyroglutamate; a = C-terminal amide. Species abbreviations: A. rub (*Asterias rubens*; Phylum Echinodermata), S. pur (*Strongylocentrotus purpuratus*; Phylum Echinoderma), H. sap (*Homo sapiens*; sub-phylum Vertebrata, phylum Chordata), C. int (Ciona intestinalis; sub-phylum Urochordata, Phylum Chordata), A. cal (*Aplysia californica*; Phylum Mollusca), P. dum (*Platynereis dumerilli*; phylum Annelida)**,** C. ele

(*Caenorhabditis elegans*; Phylum Nematoda), A. gam (*Anopheles gambiae*; Phylum Arthropoda).

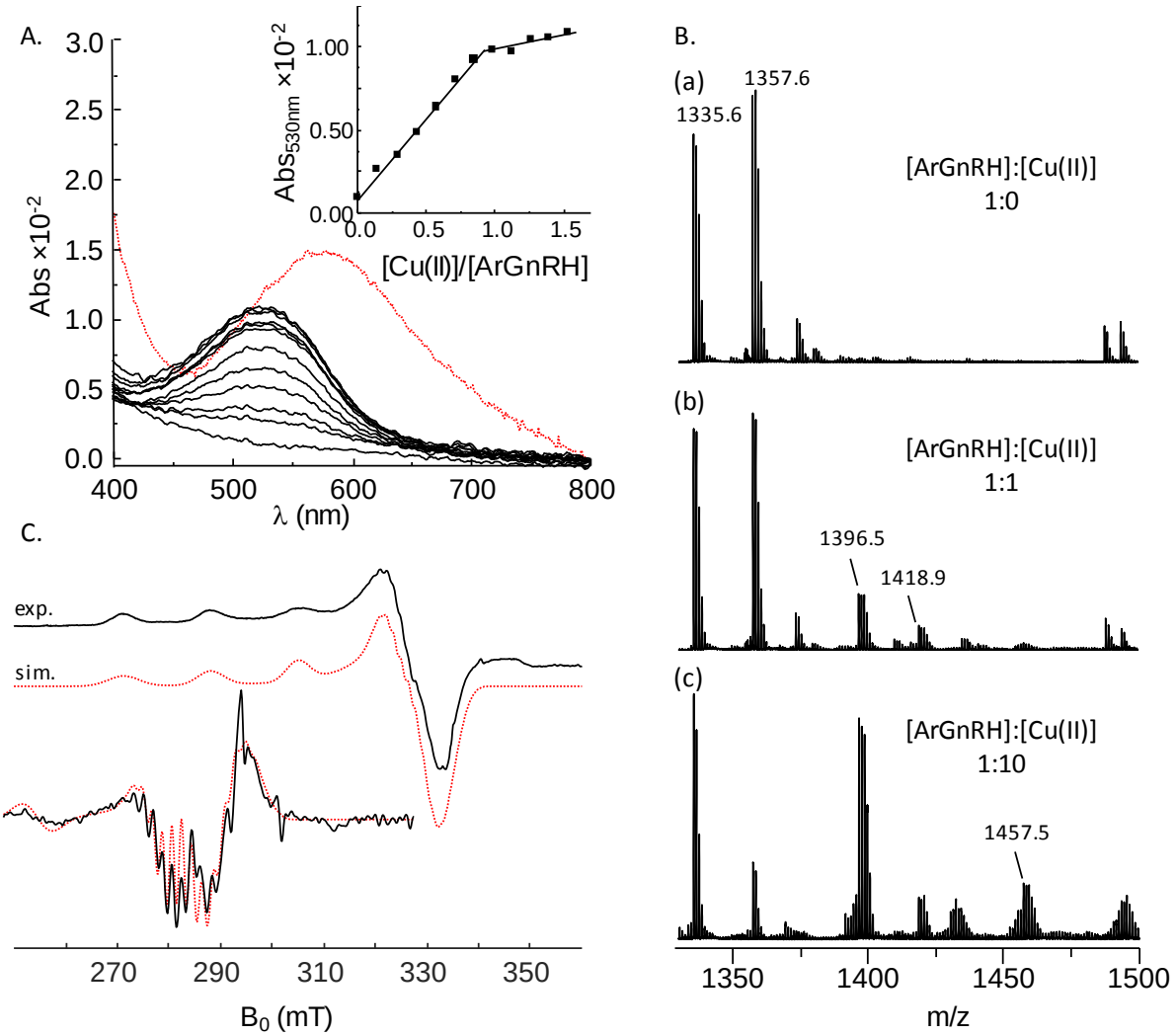
A.
Abs ×10-2
λ (nm)
Abs530nm ×10-2
[Cu(II)]/[ArGnRH]
B.
(a)
1357.6
1335.6
[ArGnRH]:[Cu(II)]
1:0
(b)
[ArGnRH]:[Cu(II)]
1:1
1396.5
1418.9
(c)
[ArGnRH]:[Cu(II)]
1:10
1457.5
m/z
C.
exp.
sim.
B0 (mT)

Figure 1.

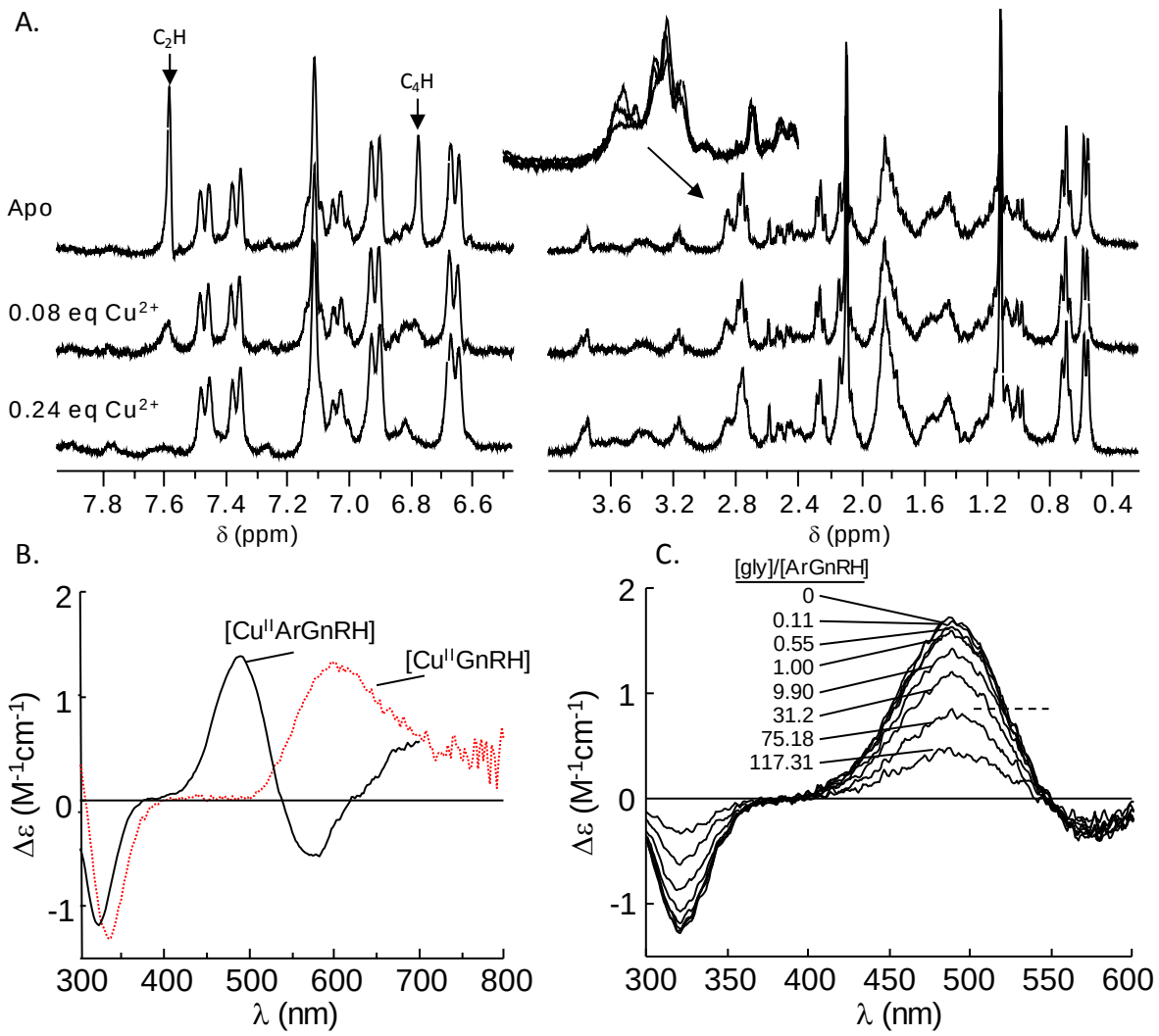
A.
C2H
C4H
Apo
0.08 eq Cu2+
0.24 eq Cu2+
7.8 7.6 7.4 7.2 7.0 6.8 6.6
δ (ppm)
3.6 3.2 2.8 2.4 2.0 1.6 1.2 0.8 0.4
δ (ppm)
B.
[CuIIArGnRH]
[CuIIGnRH]
Δε (M-1cm-1)
λ (nm)
C.
[gly]/[ArGnRH]
0
0.11
0.55
1.00
9.90
31.2
75.18
117.31
Δε (M-1cm-1)
λ (nm)

Figure 2

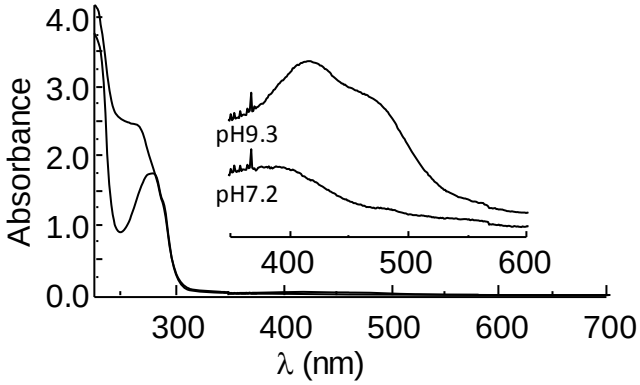
4.0
3.0
2.0
1.0
0.0
Absorbance
pH9.3
pH7.2
400
500
600
300
400
500
600
700
λ (nm)

Figure 3

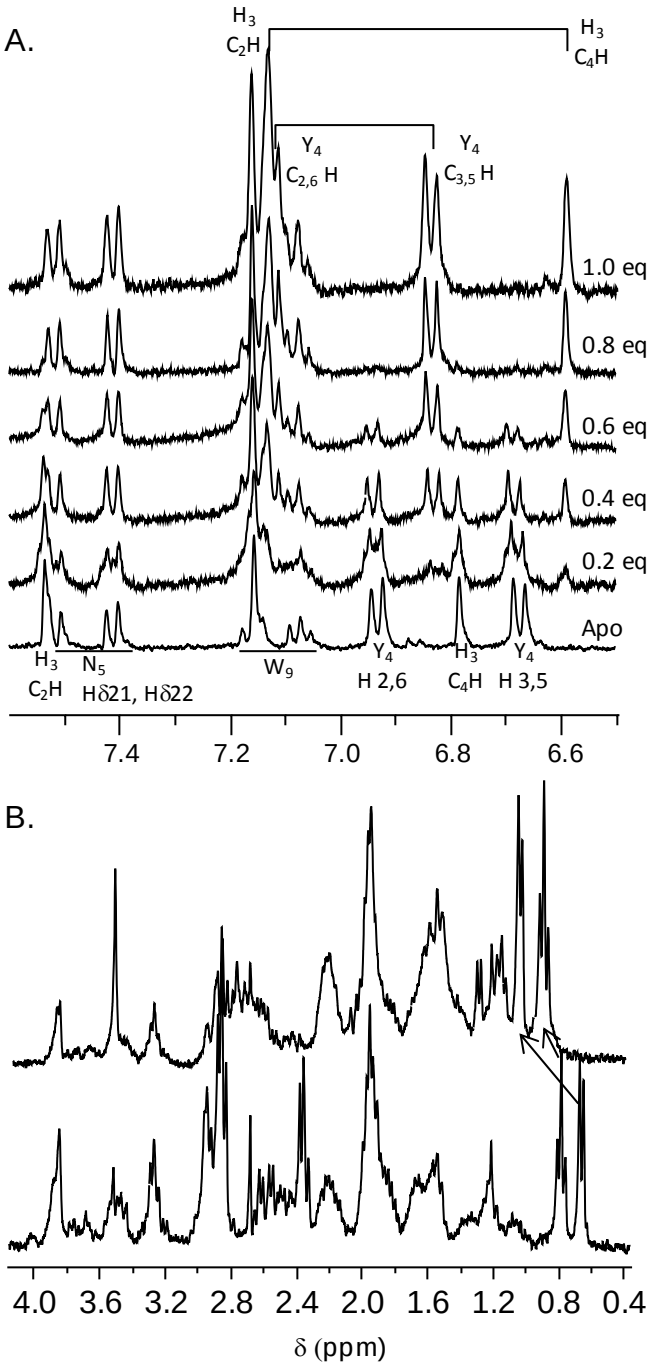
A.
H3 C2H
H3 C4H
Y4 C2,6 H
Y4 C3,5 H
1.0 eq
0.8 eq
0.6 eq
0.4 eq
0.2 eq
Apo
H3 C2H
N5 Hδ21, Hδ22
W9
Y4 H 2,6
H3 C4H
Y4 H 3,5
7.4
7.2
7.0
6.8
6.6
B.
4.0
3.6
3.2
2.8
2.4
2.0
1.6
1.2
0.8
0.4
δ (ppm)

Figure 4

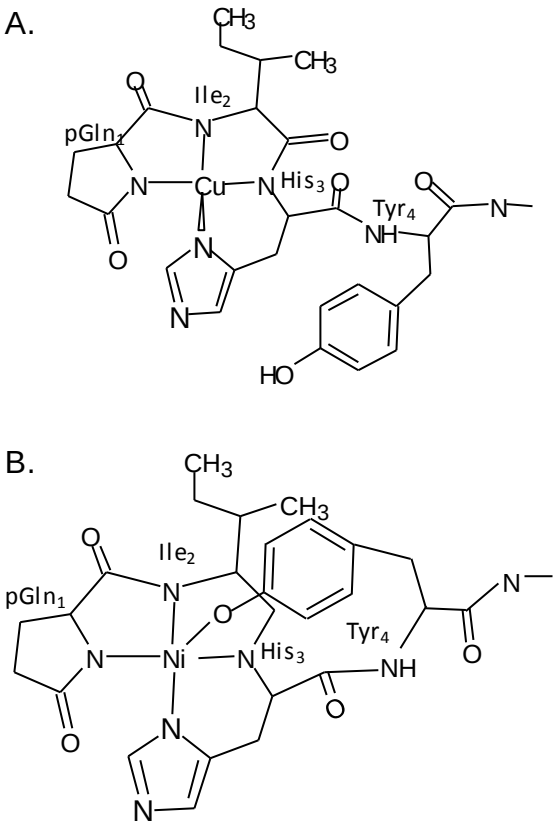
A.
CH3
CH3
Ile2
pGlu1
N
O
O
N
Cu
N
His3
O
O
Tyr4
NH
N
O
N
N
HO
B.
CH3
CH3
Ile2
pGlu1
N
O
O
N
O
Tyr4
N
Ni
N
His3
NH
O
O
N
N

Figure 5

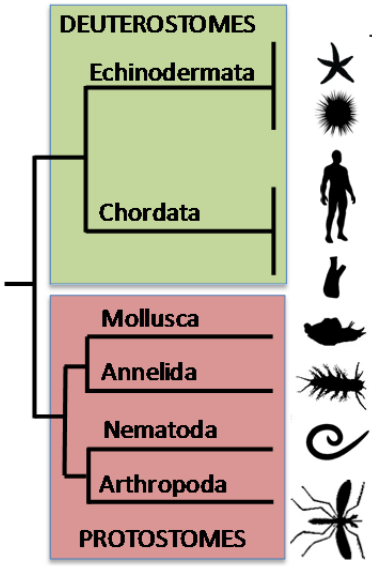

		12345	Copper binding (K_d, Ref.)
A. rub	GnRH	pQIHYKNPG-WGPGa	Yes (~10^{-12} M, this work)
S. pur	GnRH	pQVHHRFSG-WRPGa	Yes*
H. sap	GnRH1	pQHWSY--G-LRPGa	Yes (~10^{-9} M, Gul *et al.*[8])
H. sap	GnRH2	pQHWSH--G-WYPGa	Yes*
C. int	GnRH1	pQHWSY--A-LSPGa	Yes (~10^{-9} M)*
A. cal	GnRH	pQIHFS-PD-WG-Ta	Yes (~10^{-12} M)*
P. dum	GnRH	pQFSFSLPGKWG-Na	No*
C. ele	GnRH	pQMTFT-DQ-W--Ta	No*
A. gam	AKH	pQLTFT-PA-W---a	No*
A. gam	ACP	pQVTFS-RD-W--Na	No*

Figure 6

Table 1.

Spin Hamiltonian parameters for [Cu^{II}ArGnRH].

Complex	g_x	g_y	g_z	$A_x^a(^{63}Cu)$	$A_y^a(^{63}Cu)$	$A_z^a(^{63}Cu)$	$A_x^a(^{14}N)$	$A_y^a(^{14}N)$	$A_z^a(^{14}N)$	Ref.
[Cu^{II}ArGnRH]	2.063	2.034	2.250	13.3	12.7	173.3	14.0	15.7	8.3	This work
[Cu^{II}GnRH]	2.045	2.045	2.207	6.67	6.67	176.7	na	na	na	Gul *et al.*[8]

[a]Units are $\times 10^{-4}$ cm^{-1}